ANL/MSD/CP-99111

58918-00-105
58701-00-105

Conf. Paper

# Exchange Bias in Fe/Cr Double Superlattices

J.S. Jiang, G.P. Felcher, A. Inomata, R. Goyette, C.S. Nelson, and S.D. Bader

*Materials Science Division*
*Argonne National Laboratory, Argonne, IL 60439*



Proc. 46th Int. Symp. of the American Vacuum Society, Seattle, WA, Oct. 25-29, 1999 (to be published by Jour. Vac. Sci. and Technol.)

Work supported by the U.S. Department of Energy Basic Energy Sciences-Materials Sciences under contract #W-31-109-ENG-38.

## DISCLAIMER

AVS'99
1338
MI-WeA2

# Exchange Bias in Fe/Cr Double Superlattices

J. S. Jiang, G. P. Felcher, A. Inomata, R. Goyette, C. S. Nelson, and S. D. Bader

Argonne National Laboratory, Argonne, IL 60439

## Abstract

Utilizing the oscillatory interlayer exchange coupling in Fe/Cr superlattices, we have constructed 'double superlattice' structures where a ferromagnetic (F) and an antiferromagnetic (AF) Fe/Cr superlattice are coupled through a Cr spacer. The minor hysteresis loops in the magnetization are shifted from zero field, *i.e.*, the F superlattice *is* exchange biased by the AF one. The double superlattices are sputter-deposited with (211) epitaxy and possess uniaxial in-plane magnetic anisotropy. The magnitude of the bias field is satisfactorily described by the classic formula for collinear spin structures. The coherent structure and insensitivity to atomic-scale roughness makes it possible to determine the spin distribution by polarized neutron reflectivity, which confirms that the spin structure is collinear. The magnetic reversal behavior of the double superlattices suggests that a realistic model of exchange bias needs to address the process of nucleating local reverse domains.

## 1. Introduction

The exchange bias effect is a magnetic pinning phenomenon at the interface between a ferromagnet (F) and an antiferromagnet (AF). It is characterized by a field-offset, or "biased", hysteresis loop after the AF is cooled to below its Ne l temperature while the F is single-domained by an applied field.[1] Although the exchange bias effect provides a means to establish a unidirectional anisotropy and has been widely utilized in magnetic field sensing/detection applications[2], its microscopic origin is still unclear.[3] In conventional exchange bias structures such as AF/F bilayers, the magnitude of the exchange bias field $H_E$ is expected to be given by balancing the gain in Zeeman energy with the energy cost of breaking the interfacial coupling when the F layer reverses its magnetization,[4] *i.e.*,

$$H_E = \frac{J_{\text{int}}}{M_F t_F} \quad , \tag{1}$$

where $J_{int}$, $M_F$, $t_F$ are the interfacial exchange coupling energy, the magnetization and the thickness of the F layer, respectively. Experimentally, the $1/t_F$ dependence of $H_E$ has been well established, confirming the interfacial nature of the exchange bias effect. The measured magnitude of $H_E$, however, is typically more than an order of magnitude smaller than estimates using atomic exchange as the interfacial coupling energy, with the exception of NiFe/FeMn bilayers grown via molecular beam epitaxy.[5]

Early models for exchange bias address this difficulty by invoking roughness-induced variations in the coupling and/or the formation of a magnetic domain wall parallel to the AF/F interface.[6,7] Recent models also take into account the interfacial spin configuration (*e.g.* compensated *vs* uncompensated AF surfaces), the polycrystallinity of real samples, and the dynamics of the magnetization process.[8-11] While these models are

successful in explaining many aspects of the exchange bias phenomenon, direct experimental verification of the assumed atomic and magnetic configurations has always been difficult. Since the interface is buried and therefore inaccessible to most surface probes, the AF spin structure at the interface is often assumed to be the same as that of the bulk, while in reality there could be a spin re-arrangement at the interface. The reduced lateral coherence due to interfacial roughness or random AF domains renders scattering experiments ineffective.[12] In view of these unresolved issues, it is beneficial to construct a system where the exchange bias effect can be realized and studied in detail with minimal material-related complexities.

The exchange coupling of ferromagnetic transition-metal layers across a non-magnetic spacer allows for the creation of magnetic structures with desired magnetic configurations.[13] Magnetic superlattices that utilize interlayer coupling can be viewed as a model one-dimensional magnetic system, where each constituent magnetic layer represents an atomic spin, and the interlayer coupling represents the inter-atomic exchange. Such a mapping essentially enlarges the basic length scale in magnetic coupling phenomena from inter-atomic distances to the layer thicknesses, easing experimental difficulties in dealing with the intransigence of atomic roughness. Furthermore, in a layered structure, it is possible to tailor the interlayer coupling and anisotropy to be comparable to the Zeeman energies associated with modest magnetic fields by choosing appropriate layer thicknesses. For example, AF-coupled Fe/Cr superlattices have been used to demonstrate the existence of the surface spin-flop transition,[14] a phenomenon which had long been predicted but never before observed experimentally.

To model the exchange bias effect at an AF/F interface, we have grown Fe/Cr *double-superlattice* structures.[15] The interlayer exchange coupling between Fe layers

across a Cr spacer oscillates between F and AF coupling with a 'long'period of 18 of Cr.[16] An Fe/Cr double superlattice is represented as $[Fe/Cr]^{4F}/Cr/[Fe/Cr]^{F}$, where the superscripts denote AF and F coupling within each superlattice. (See inset of Fig. 1a) The double superlattices are grown epitaxially onto single-crystal MgO(110) substrates, resulting in (211)-orientation and an in-plane uniaxial anisotropy. The easy magnetization direction is along the Fe/Cr $[0\bar{1}1]$, and the strength of the uniaxial anisotropy is inversely proportional to the Fe layer thickness.[17] The inter-superlattice coupling is governed by the thickness of the center Cr layer. Thus, Fe/Cr double superlattices offer tunable coupling and anisotropy strength. The 18- period of the oscillatory interlayer coupling is relatively long compared to the range of the inter-atomic exchange in conventional AF/F interfaces. Hence, the coupling between the AF and F superlattices in double-superlattice structures is less sensitive to atomic-scale thickness fluctuations and can be considered as being uniform across the interface. The layered structure is also ideal for polarized neutron reflectivity (PNR) studies since 18 is well within the instrumental resolution. Owing to the coherent structure of the double superlattices, we are able to carry out spin-dependent neutron reflectivity measurements[18] that give information about the magnetic and structural profile perpendicular to the AF/F interface.

## 2. Experiment

The epitaxial Fe/Cr double-superlattices were grown via dc magnetron sputtering onto single-crystal MgO(110) substrates under conditions similar to those reported previously.[17] A 200- Cr buffer layer was first deposited at 400¡C to establish epitaxy with the substrate. The double-superlattice structure was then grown at 100¡C, followed by a 50- Cr cover layer. The configuration of the AF superlattice is $[Fe_{14}/Cr_{11}]_{20}$, and

that of the F superlattice is $[Fe_{50}/Cr_{20}]_{n_F}$ with $n_F$ = 1, 2, 3, 5, and 10. The subscripts inside the brackets denote the layer thicknesses and the ones outside denote the number of bilayer repetitions. The Cr layer between the AF and F superlattices is 20 thick and gives rise to ferromagnetic inter-superlattice coupling. Samples with only one AF or F superlattice were also prepared similarly for comparison.

The structures were characterized by x-ray diffraction using Cu $K_\alpha$ radiation. High-angle superlattice peaks up to the third order were observed. Fittings to the low angle x-ray reflectivity yield an rms roughness at Fe/Cr interfaces of ~6 , [19] and asymmetric $\phi$-scans show the expected in-plane epitaxial relations: Fe/Cr[0$\bar{1}$1]||MgO[001] and Fe/Cr[$\bar{1}$11]||MgO[1$\bar{1}$0]. The magnetization was measured in a SQUID magnetometer at temperatures ranging from 4.5 to 295 K with the field applied along the easy axis. Minor magnetization loops were taken by first saturating the samples in a 20 kOe field. The room-temperature minor loops were also measured using the longitudinal magneto-optic Kerr effect (MOKE). To correct for remanent fields due to trapped flux each time the superconducting magnet of the SQUID magnetometer was charged to a high field, a second minor loop was measured with the sample rotated by 180¡. The midpoint between centers of the two minor loops defines the true zero field point. The remanent field values agree with those determined by measuring the magnetization of a paramagnetic Pd standard. PNR measurements for a double superlattice with $n_F$ = 5 were taken at the instrument "POSY I" at the Pulsed Neutron Source of Argonne National Laboratory.

### 3. Results and Discussion

Shown in Fig. 1a is the room-temperature magnetization curve of a double

superlattice with $n_F$ = 5 measured by SQUID magnetometry. The magnetization is normalized with respect to the full saturation value. Since the Fe moment in the F superlattice comprises 47% of the total moment and the AF superlattice contributes zero net magnetization, the transition between +0.47 and -0.47 in the normalized magnetization in low fields represents magnetic reversal of the F superlattice. The kinks in magnetization marked by arrows identify the spin-flop transitions in the AF superlattice.[14] With increasing field, the Fe moments in the AF rotate from a spin-flopped state toward parallel alignment and the magnetization gradually increases. The field values for the spin-flop transition (2 kOe) and for saturation (14 kOe) are the same as those reported in Ref. 17 for AF superlattices with the same layer thicknesses. The anisotropy constant of 0.06 erg/cm$^2$ determined from the hard-axis magnetization curves also is in agreement with the previously published value. Hence, from the structural and magnetic characterizations, we can conclude that the samples in this study are comparable in quality to those in Ref. 17.

In a conventional AF/F exchange bias system, cooling in a field through the Ne l temperature of the AF is required to establish a unidirectional anisotropy. However, this is not necessary for our AF/F double-superlattices. Figure 1b shows the minor hysteresis loop of the same double-superlattice measured in fields between +200 Oe and -200 Oe, after a large field $H_A$ = +20 kOe had been applied to align all the Fe layers. The magnetization is normalized with respect to the full saturation value. Since the Fe moment in the F superlattice comprises 47% of the total moment and the magnetization switches between 0.47 and —0.47in this field range, the minor loop represents the magnetization behavior of the F superlattice. The center of the minor loop is shifted to the negative field direction by an amount $H_E$ = 34.4 Oe. The shifted hysteresis loop

manifests a unidirectional anisotropy. The aligning field breaks the symmetry between two energetically equivalent AF states and leaves the interfacial Fe layer in the AF superlattice necessarily parallel to the alignment direction. This is equivalent to field cooling in conventional systems. To overcome the exchange interaction between the F and the interfacial Fe layer in the AF, an additional field in the negative direction is needed. Therefore the hysteresis loop of the F superlattice appears shifted toward the negative field direction. Note that the width of the hysteresis loops is only ~10 Oe, which is much smaller than the anisotropy field. *This indicates that in these double superlatttices the magnetization reversal of the F superlattice is not by coherent rotation, but rather by nucleation and growth of reverse magnetic domains.* Also shown in Fig. 1b is the minor loop measured using MOKE. Since the Kerr effect is sensitive to the magnetization on the scale of the optical penetration depth (~200 ) which is roughly the thickness of the F superlattice, the single-stepped switching in Kerr intensity indicates that all of the Fe layers in the F reverse their magnetization simultaneously. The sharpness of the switching also indicates pinning-free domain wall motion. Therefore, the exchange coupling manifests itself as a bias field at the onset of domain reversal. It is worth noting that most exchange bias models imply a coherent rotation of the F magnetization.[6,7-8,10] A scenario of nucleation and growth of reverse domains in exchange bias systems is discussed only indirectly in Ref. 9. The double superlattices studied here have AF/F coupling strength comparable to those in conventional exchange bias systems. This suggests that a realistic model of exchange bias needs to address the process of nucleating local reverse domains.

In Fig. 2, the values of the exchange bias field $H_E$ for several double-superlattices are shown as a function of $n_F$. With increasing $n_F$, $H_E$ decreases monotonically. The

magnitude of the exchange bias field for a collinear spin configuration is given by Eq. 1. In the double superlattices, the equivalent interfacial exchange interaction is the coupling across the center Cr layer, and $t_F M_F = n_F d_{Fe}^F M_{Fe}$, where $d_{Fe}^F$ is the Fe layer thickness in the $F$ superlattice and $M_{Fe}$ the saturation magnetization of Fe. We calculated the exchange bias field from Eq. 1 and plot it as the solid curve in Fig. 2. In order to do this we used $d_{Fe}^F = 50$ , $M_{Fe} = 1700$ emu/cm$^3$, and $J_F = 0.07$ erg/cm$^2$. The latter value was reported previously for the interlayer coupling across 20 of Cr,[17] noting that $J_{int} = 2J_F$ since $J_F$ was originally defined per Fe layer in a bilayer structure.[20] Such a comparison is possible only because the high-quality AF/F interfaces in our double superlattices permit unambiguous determination of $J_{int}$. Note that whereas the bias field in conventional AF/F systems is about two orders of magnitude smaller than that given by Eq. 1, the data points in Fig. 2 are well-described by the calculated curve.

Figure 3 shows the temperature dependence of the bias field $H_E$ and coercivity $H_C$ for the $n_F = 5$ double superlattice. $H_E$ increases with decreasing temperature. The thermal variation of the interlayer exchange coupling energy has the form[21]:

$$J_1(T) = J_1(0)\frac{T/T_0}{\sinh(T/T_0)}. \qquad (2)$$

Least-square fitting of the data in Fig. 3 gives $J_1(0) = 0.196$ erg/cm$^2$ and $T_0 = 218.6$ K for the 20- Cr spacer. The coercivity, however, does not show discernible temperature dependence. This should be contrasted to conventional exchange bias systems where the temperature dependence of $H_E$ is correlated with the variation in the density of interfacial uncompensated spins,[22] and where $H_C$ shows a concomitant variation with $H_E$. It has been pointed out that one contributing factor to coercivity in conventional exchange bias systems is the instability of the AF grains[10] and local variations of the AF anisotropy.[23]

Since such inhomogeneities are precisely what are avoided here, the lack of temperature dependence for $H_C$ is consistent with the absence of this coercivity mechanism in the double superlattices.

Polarized neutron reflectivity measurements were taken in order to determine the layer-by-layer magnetization of the double superlattice, both in size and orientation. Two scans were taken at room temperature in the two branches of a minor loop after aligning the sample. They were, respectively, at -21 Oe with the ferromagnet magnetized in the direction of the aligning field; and at -35 Oe after cycling to -120 Oe, where the ferromagnet is magnetized in the opposite direction. Figure 4 shows the reflectivities for neutrons polarized parallel ($R_+$) and antiparallel ($R_-$) to the applied field H = -35 Oe, as a function of the perpendicular momentum transfer $q_z = 4\pi \sin\theta / \lambda$, where $\theta$ is the angle of the neutron beam with respect to the surface plane, and $\lambda$ is the neutron wavelength. It is interesting to describe the physical significance of the main features of the spectra. The strong spin dependence of the reflectivity indicates the presence of large magnetic induction fields in the sample, parallel to the applied field. At the left side of Fig. 4, the critical angle is characteristic of the MgO substrate, while at the right side, the broad ferromagnetic peak appears (the first AF peak is out of the $q_z$ range presented here). The most pronounced interference fringes of the + polarized neutrons correspond to the total thickness of the F superlattice. Also indicated in Fig. 4 is the reflectivity calculated assuming a *collinear* distribution of the spins of the F and the AF components ——with the magnetization of the first AF layer opposite to that of the F superlattice. The spin asymmetry, $P = (R_+ - R_-)/(R_+ + R_-)$, is shown in Fig. 5 for the two magnetization branches. The measurements show a pronounced difference at $q_z$ = 0.05. This is the region where the calculated asymmetries are most sensitive to the reversal of the

magnetization in the F superlattice. Since non-collinear configurations do not contribute to the asymmetry (the relevant magnetic and nuclear amplitudes are in quadrature), this result provides the most direct confirmation hitherto obtained of a collinear spin configuration in an exchange bias system.

## 4. Summary

In conclusion, we have demonstrated exchange bias behavior in a novel Fe/Cr(211) double-superlattice structure that utilizes oscillatory interlayer exchange coupling. The exchange-bias field agrees quantitatively with the classical formula for collinear spin structures. Polarized neutron reflectivity analysis confirms the collinear spin distribution. While there is no straightforward way to characterize and manipulate the interfacial coupling in conventional exchange bias systems, our double-superlattice structures have coherent AF/F interfaces. The flexibility in configuration, and tunable coupling strength and magnetic anisotropy offered by the double-superlattice structures should create new opportunities to elucidate the underlying physics of the exchange bias phenomenon.

## Acknowledgement

This work was supported by the U.S. Department of Energy, BES-MS under contract 31-109-ENG-38.

**References:**

1. W. H. Meiklejohn and C. P. Bean, Phys. Rev. 105, 904 (1957).

2. C. Tang, J. Appl. Phys. 55, 2226 (1984); B. Dieny, V. S. Speriosu, S. S. P. Parkin, D. R. Wilhoit_ and D. Mauri, Phys. Rev. B 43, 1297 (1991).

3. J. Nogu s and I. K. Schuller, J. Magn. Magn. Mater. 192, 203 (1999), and references therein.

4. W. H. Meiklejohn, J. Appl. Phys. 33, 1328 (1962).

5. R. Jumgblut, R. Coehoorn, M. T. Johnson, Ch. Sauer, P. J. van der Zaag, A. R. Ball, T. G. S. M. Rijks, J. aan de Stegge, and A. Reinders, J. Magn. Magn. Mater. 148, 300, (1995).

6. D. Mauri, H. C. Siegmann, P. S. Bagus, and E. Kay, J. Appl. Phys, 62, 3047 (1987).

7. A. P. Malozemoff, Phys. Rev. B_35, 3679 (1987).

8. N. C. Koon, Phys. Rev. Lett. 78, 4865, (1997).

9. T. C. Schulthess and W. H. Bulter, Phys. Rev. Lett. 81, 4516, (1998).

10. M. D. Stiles and R. D. McMichael, Phys. Rev. B 59, 3722, (1999).

11. R. E. Camley, B. V. McGrath, R. J. Astalos, R. L. Stamps, and Joo-Von, J. Vac. Sci. Technol. (in press).

12. S. S. P. Parkin, V. R. Deline, R. O. Hilleke, and G. P. Felcher, Phys. Rev. 42, 10583 (1990); G. P. Felcher, Y. Y. Huang, M. Carey, and A. E. Berkowitz, J. Magn. Magn. Mater, 121, 105, (1993).

13. S. S. P. Parkin and D. Mauri, Phys. Rev., B 44, 7131 (1991).

[14]. R. W. Wang, D. L. Mills, E. E. Fullerton, J. E. Mattson, and S. D. Bader, Phys. Rev. Lett. 72, 920, (1994).

[15]. J. S. Jiang, G. P. Felcher, A. Inomata, R. Goyette, C. S. Nelson, and S. D. Bader (submitted).

[16]. S. S. P. Parkin, N. More, and K. P. Roche, Phys. Rev. Lett. 64, 2304, (1990); J. Unguris, R. J. Celotta, and D. T. Pierce, Phys. Rev. Lett. 67, 140 (1991).

[17]. E. E. Fullerton, M. J. Conover, J. E. Mattson, C. H. Sowers, and S. D. Bader, Phys. Rev. Lett. 48, 15755 (1993); E. E. Fullerton, M. J. Conover, J. E. Mattson, C. H. Sowers, and S. D. Bader, J. Appl. Phys. 75, 6461 (1994).

[18]. H. Zabel, Physica B, 198, 156 (1994).

[19]. S. G. E. te Velthuis, G. P. Felcher, J. S. Jiang, A. Inomata, C. S. Nelson, A.Berger and S. D. Bader (submitted).

[20]. W. Folkerts, J. Magn. Magn. Mater, 94, 302 (1991).

[21]. P. Bruno, Phys. Rev. B 52, 411 (1995).

[22]. K. Takano, R. H. Kodama, A. E. Berkowitz, W. Cao, and G. Thomas, Phys. Rev. Lett. 79, 1130 (1997).

[23]. V. I. Nikitenko, V. S. Gornakov, L. M. Dedukh, Yu. P. Kabanov, A. F. Khapikov, A. J. Shapiro, R. D. Shull, A. Chaiken, and R. P. Michel, Phys. Rev. B 57, R8111 (1998).

**Figure Captions:**

Fig. 1 Room-temperature magnetization curve of an $[Fe_{14}/Cr_{11}]_{20}/Cr_9/[Fe_{14}/Cr_{11}]_{20}$ double superlattice. The arrows mark spin flop transitions. Inset: Schematic illustration of a double-superlattice structure. The dark layers represent magnetic layers. (b) Minor hysteresis loops of the same Fe/Cr double superlattice after alignment at +20 kOe. The solid line is SQUID magnetometry measurements and the dash lines is for the magneto-optic Kerr effect. The magnetization is normalized to the full saturation value.

Fig. 2: The exchange bias field $H_E$ as a function of the number of Fe layers in the $F$ superlattice, $n_F$. The solid curve is the calculated exchange bias field as described in the text.

Fig. 3: Temperature dependence of the exchange bias field $H_E$ (squares) and the coercivity $H_C$ (circles) of the double superlattice of Fig. 1. The solid curve is a fit as described in the text, the dashed line is a guide to the eye.

Fig. 4: Measured and calculated polarized neutron reflectivity for the double superlattice of Fig. 1 in a field H = -35 Oe for neutrons with spin parallel to H (full points/full line) and antiparallel to H (open points/dashed line).

Fig. 5: Top: Spin asymmetry P for the double superlattice of Fig. 1 in a descending field of H = -21 Oe. Bottom: -P for the same sample in an ascending field H = -35 Oe. The curves are calculations assuming a collinear spin profile. The diagrams illustrate the spin configurations near the AF/F interface. The parallel arrows indicate the magnetization directions of the Fe layers in the F superlattice and the antiparallel arrows indicate those in the AF superlattice.

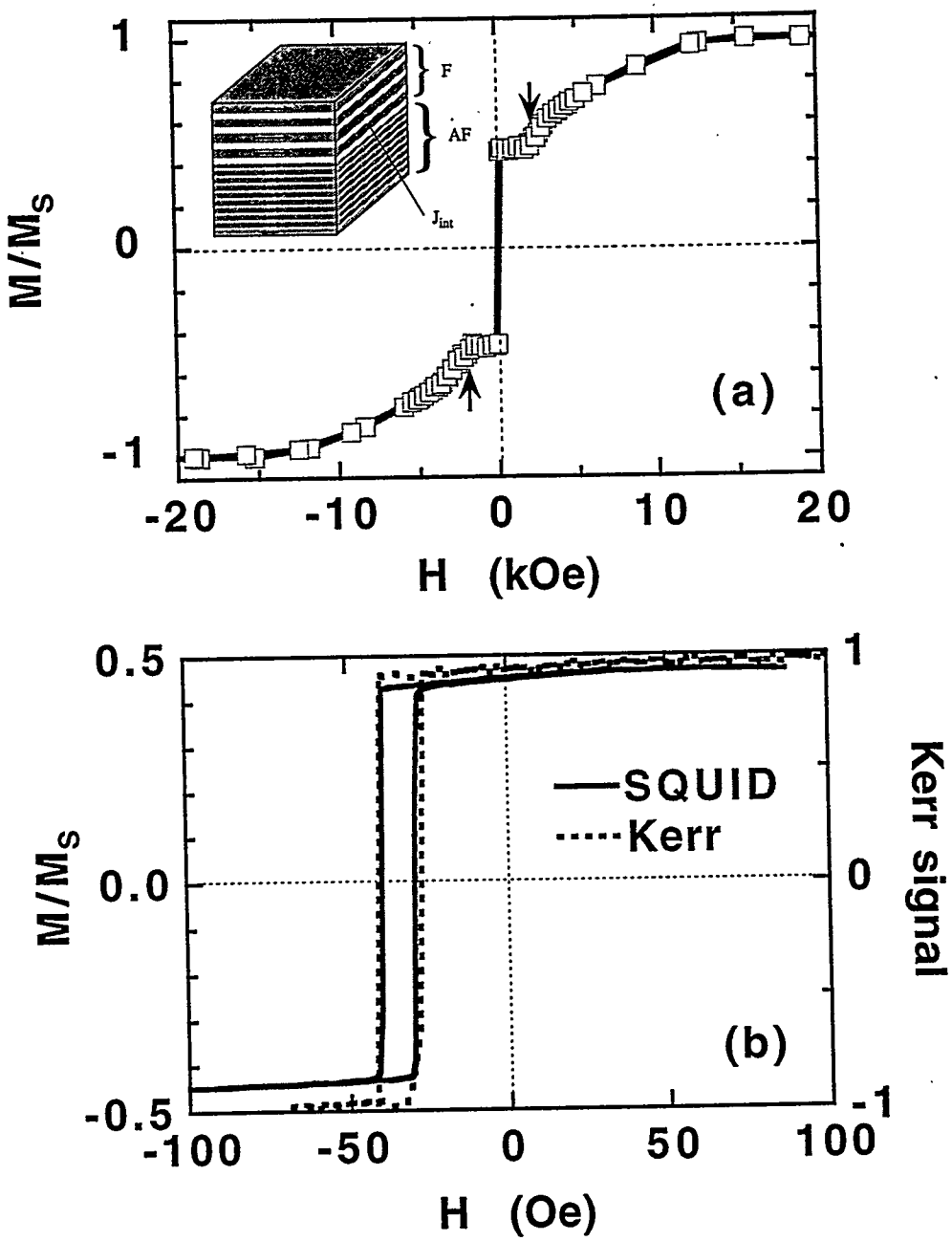
1
0
-1
M/M$_S$
F
AF
J$_{int}$
(a)
-20
-10
0
10
20
H (kOe)
0.5
0.0
-0.5
M/M$_S$
SQUID
Kerr
(b)
1
0
-1
Kerr signal
-100
-50
0
50
100
H (Oe)

Figure 1

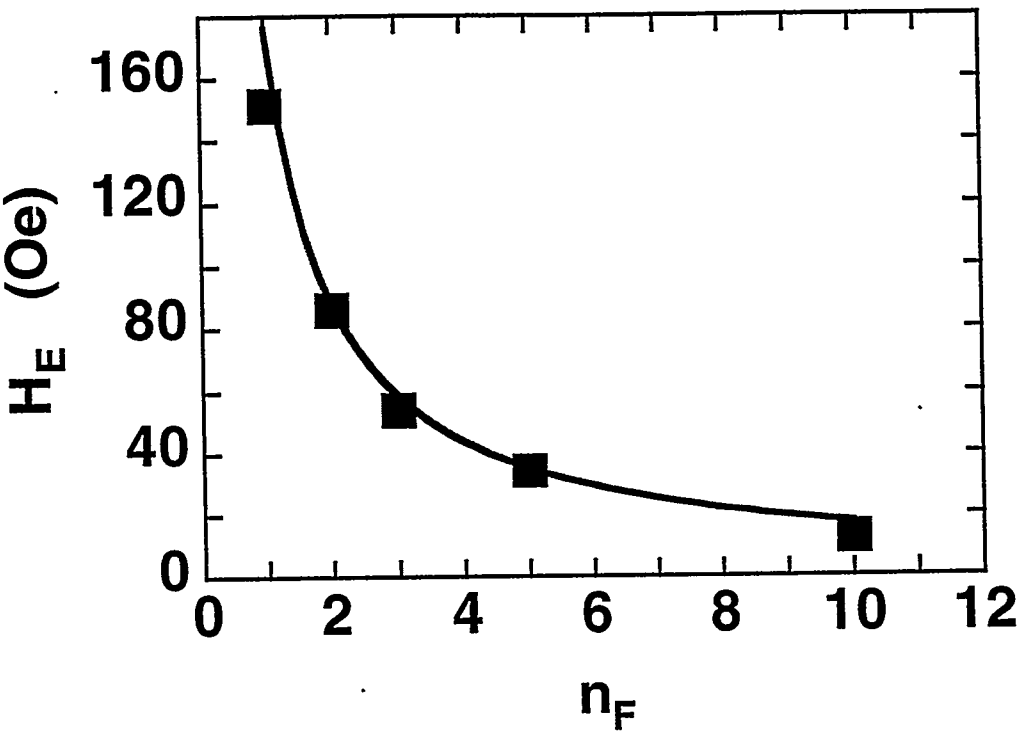


Figure 2

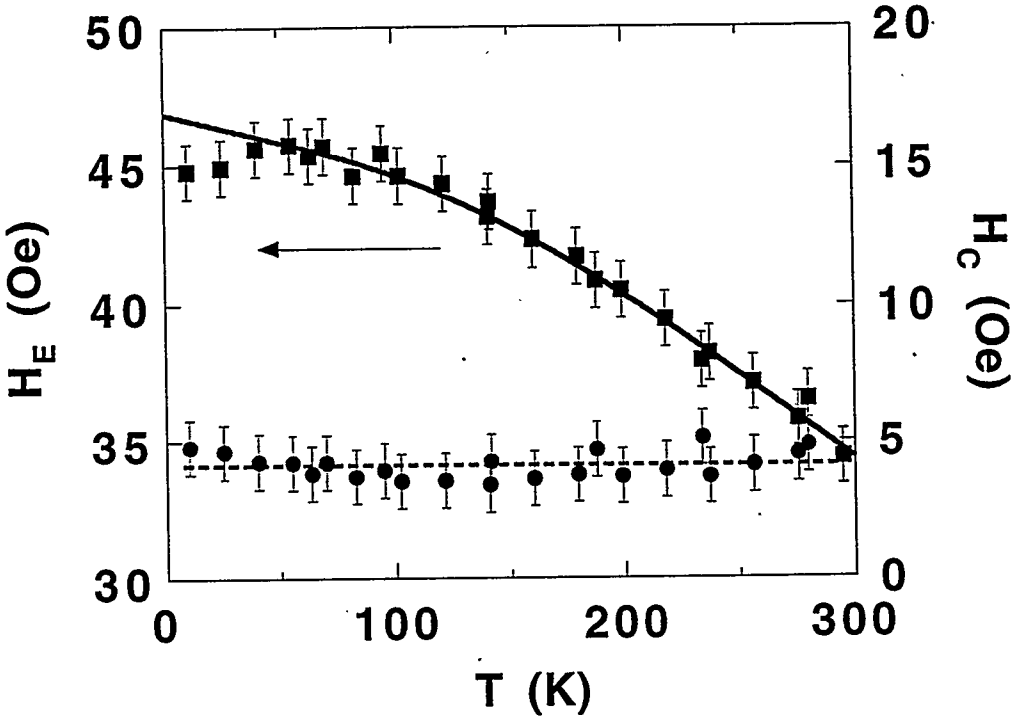


Figure 3

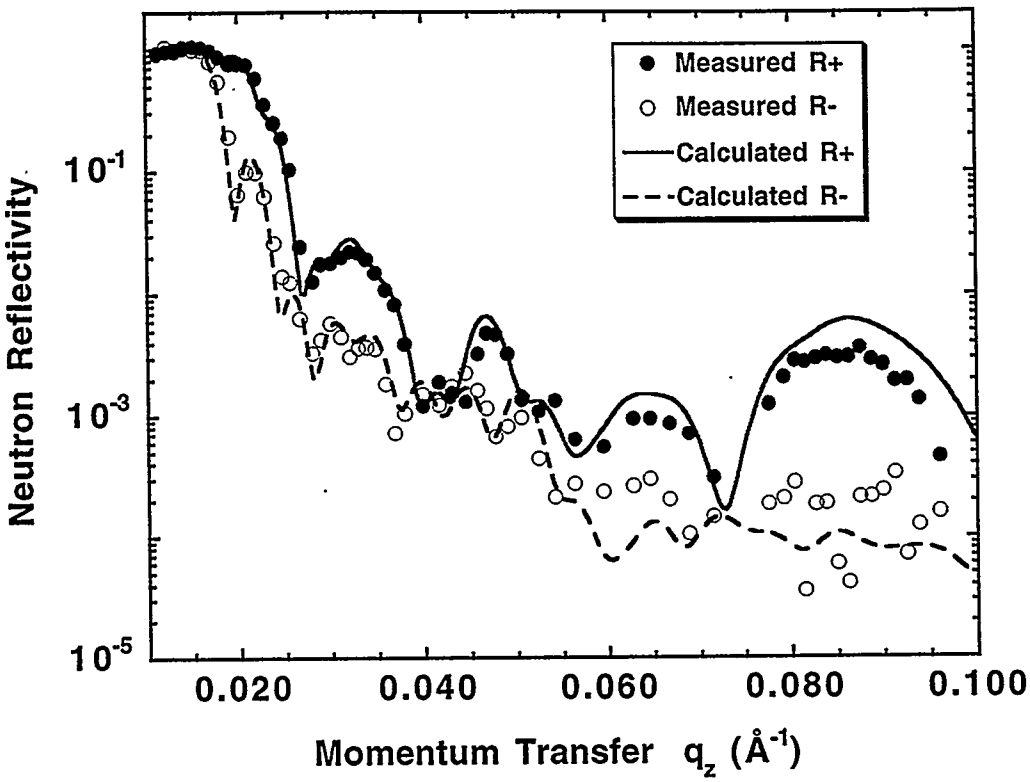
Measured R+
Measured R-
Calculated R+
Calculated R-
Neutron Reflectivity
$10^{-1}$
$10^{-3}$
$10^{-5}$
0.020
0.040
0.060
0.080
0.100
Momentum Transfer $q_z$ (Å$^{-1}$)

Figure 4

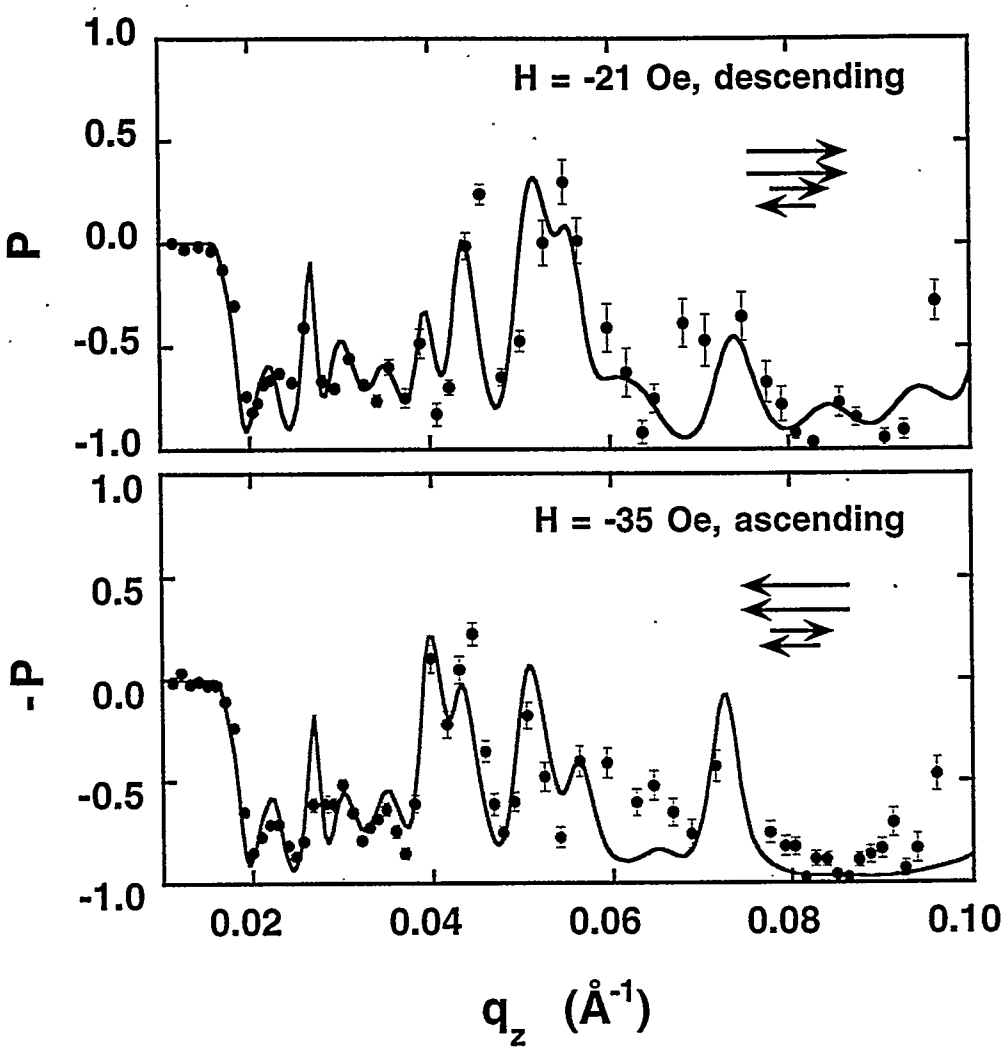
H = -21 Oe, descending
H = -35 Oe, ascending
P
-P
1.0
0.5
0.0
-0.5
-1.0
0.02
0.04
0.06
0.08
0.10
$q_z$ (Å$^{-1}$)

Figure 5